

Energy Conditioning for Implantable Medical Devices: A Multiple Input Redundant System

Ana Marta Carpinteiro de Barros Borges
Instituto Superior Tecnico (IST)
Lisbon, Portugal
anamartaborges@tecnico.ulisboa.pt

Abstract—Powering up implantable medical devices (IMDs) by taking advantage of energy harvesting devices, which convert energy collected from human body activities into electrical energy, has been increasingly an alternative to fixed density and lifetime batteries, that may represent several drawbacks for patients. Piezoelectric and electrostatic generators gather the best results in terms of output power generated and reliability. In order to combine these energy harvesters characteristics, there are several approaches that have multiple energy harvesting devices as input sources. Despite of IMDs are usually low power devices, the energy generated by energy harvesters is not enough to power them. Therefore, it is needed to boost the generated voltage, using voltage elevation circuits for this purpose.

In this work, a system capable of processing harvest energies to power up an implantable medical device that, being very simple, automatically guarantees the existence of a working input power source, was developed. It was proved that this system, besides providing some voltage elevation, is capable of readjusting the input source, maintaining the minimum output voltage required. Also, as goal, a substantial revision of the literature the energy harvesting state of the art was performed, in order to gather the relevant latest information spread by a varied literature (medical, physics, electrical and technological publications).

Index Terms—energy harvesting, implantable medical devices, boost DC-DC converter, multiple input sources system

I. INTRODUCTION

The growing need of powering electronic devices with everlasting batteries has made energy harvesting a subject with increasingly interest of study. Energy harvesting consists of scavenging energy from a source and then converting the harvested energy into electrical energy capable of powering an usually small and low power device.

Although most of implantable medical devices have low power requirements, the output power generated from energy harvesting systems may not be sufficient to efficiently power IMDs. So the output voltage must be increased using voltage elevation circuits, such as DC-DC converters, and eventually gather the contribution of several sources. However, when using these generators, their continuous working status cannot always be assured. Which means that, if one input source fails and there's no other source able to replace it, the whole system will probably fail as well, compromising the functioning of the IMD or even leading to its failure.

The main goal of this project is to develop a system capable of permanently assuring the power of an implantable medical device, using more than one energy harvesting device for collecting energy from human body activities.

The main goal of this project is to develop a system capable of permanently assuring the power of an implantable medical device, using more than one energy harvesting device for collecting energy from human body activities.

To achieve the main objective, several goals have to be established, such as the performance of a survey of the energy harvesting methods that are presently used in biomedical applications, as well as the execution of a comparative analysis to infer which methods gather the best characteristics to be implemented in the context of this projects system. This survey is also intended to be a tutorial study in what concerns the energy scavenging. After having the input energy sources, it is needed to implement a voltage elevation circuitry, since the output voltage generated by the energy harvesters is not enough to power an implantable medical device, and it is also needed to dimension a system capable of guarantee the existence of one working input source.

II. STATE OF THE ART

A. Energy Harvesting for Implantable Medical Devices

There are several sources of energy to harvest, since the human body represents an excellent source of energy produced through normal actions and physical activities, to environmental sources, such as solar and infrared energy. The process of energy harvesting requires, apart from an energy source, a small device capable of converting the energy that has been scavenging into electrical energy. The systems that can implement energy harvesting methods are divided in two types: independent systems, which dont need an external unit to produce power and systems with external unit, which obtain the power from an external unit, through energy transfer, such as Radio Frequency transmission, inductive coupling and ultrasonic transducers. However, the use of energy transmission systems requires an external unit which has several disadvantages, such as the distance dependence between the transducer and the implant, side effects caused by transmission techniques and large size. These disadvantages make the use of this type of systems improper in the context of this project, so the following analysis will be focused on independent systems only.

Table I compares the several harvesting techniques, generated power, the size of the devices and its advantages and disadvantages.

TABLE I
COMPARISON OF INDEPENDENT SYSTEM APPROACHES FOR HARVESTING ENERGY TO POWER IMD.

Approach	Generated Power	Size	Author, Reference	Advantages	Disadvantages
Biofuel Cell	2.4 W	-	Mano, [1]	Biological compatibility	Lifetime Output power
Thermoelectric Generators	5 mV up to 25 mV 4.6 W up to 24.4 W	20 x 20 x 3 mm 58.9 mm ²	Yang, [2] Nagel, [3]	Unlimited lifetime	Reliability Biocompatibility issues
Electromagnetic Generators	22.1 J 1.1 mW 1.9 mJ	- 27.8 cm ² 3.76 cm ²	Luciano, [4] Nasiri, [5] Morais, [6]	Unlimited locations	Complex fabrication technologies
Electrostatic Generators	36 W 58 W 80 W	50 x 30 x 30 mm - -	Tashiro, [7] Tashiro, [8] Miao, [9]	High output power	Additional power source High output impedance
Piezoelectric Generators	4 mW 80 W 100 W	10 x 10 x 4 mm 5 x 5 x 18 mm 17 x 7 x 5 mm	Almouahed, [10] Lewandowski, [11] Deterre, [12]	High output power No additional voltage source	Limited implantable locations Biocompatibility issues
Subcutaneous Photovoltaic Cell	2.58 W	1.54 mm ²	Chen, [13]	Unlimited power source	Low output power

Comparing the several methods presented, it is possible to conclude that piezoelectric and electrostatic generators gather the best characteristics among all approaches for the implantable medical devices context. Piezoelectric generators present the best results in terms of generated output power and electrostatic generators, besides the good results of generated output power, their localization is almost limitless, since they do not need large amounts of force.

In order to take advantage of both output power generators, combining their advantages instead of dispensing one for the other, it has been considered the possibility of combining several approaches, resulting in a system with multiple energy harvesters as input power sources.

B. DC-DC Converters for Voltage Elevation

Although most of implantable medical devices have low power requirements, the output power generated from energy harvesting systems may not be sufficient to efficiently power IMD, in spite of using only one or multiple energy harvesters as input power sources. Consequently, as the output voltage generated is in the μV or mV order, it must be increased using voltage elevation circuits, such as DC-DC converters.

Collecting power from multiple energy sources can increase the reliability of the system and enables the combination of advantages of different sources with different voltage and current characteristics for optimal energy and economic use. Multiple input (MI) converters have been proposed and they can implement two different configurations: i) combining various input energy sources in parallel and ii) connecting the input voltage sources in series, to supply power simultaneously.

There are several examples of input voltage sources in parallel, such as the one reported by Khaligh *et al.* [14] or Chen *et al.* [15] and in parallel, such as the one that Kumar *et al.* developed in [16] or the one by Deihimi *et al.* [17].

Depending on the final application of the converter, series or parallel input power sources configuration may be more

or less suitable. Although parallel configuration can have the disadvantage of only one input source contribute at a time and consequently the output voltage is not as high as with a series configuration with simultaneously contributions, it has the advantage of when an input source is disconnected the system is able to continue working by using another input source.

III. PROPOSED SOLUTION

According to the goals of this work, for creating a redundant system capable of harvesting energy to power up an implantable medical device that always guarantees the existence of a working input power source, there are some aspects that have to be considered. First, the goal of the DC-DC converter is input voltage boosting, so a boost DC-DC converter must be used. Secondly, the system must be as simple as possible, once it will be implanted in human body, so it has been adopted a simple approach that consists in using a system with multiple input power sources with boost DC-DC converters without using additional control systems. This way, it is possible to boost each input contribution at a time to achieve a certain output voltage and when an input source is disconnected, other input source starts automatically working to guarantee the required output voltage. The block diagram of the proposed circuit for two input power sources is represented in Figure 1.

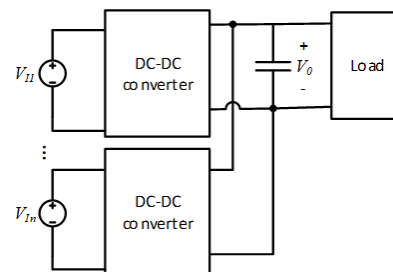


Fig. 1. Block diagram of the proposed circuit.

This system is intended to be set between a first voltage elevation circuit, if needed, and the IMD. Since the energy harvesters are able to generate only μW or mW of output power, it is needed to boost it before applying it to the proposed redundant system. This way, it is correct to say that this system is seen by the IMD as its battery.

A. Working Principle Analysis

The proposed circuit topology in this thesis consists in multiple parallel boost DC-DC converters sharing the same load. For the simplicity of the analysis, only two converters will be considered and the goal is to predict the simultaneous functioning, considering the different operation modes for both converters.

However, for best understanding the multiple converter functioning, a single converter steady state summarized analysis will be presented first.

1) *Single Converter Working Principle*: Considering firstly the individual working principle for one converter, this is an ordinary boost DC-DC converter and as represented in Figure 2, it's circuit is constituted by a coil L , a switch S , a diode D_1 and a capacitor C . The switch is periodically opened and closed, being controlled with a switching frequency of $f_{sw} = \frac{1}{T}$, where T represents the period.

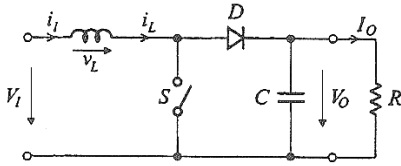


Fig. 2. Boost converter schematics [18].

The duty cycle, D , represents the time fraction the switch is closed and the output is high during one complete working period, and it can take values between 0 and 1.

When the switch is closed, the current will flow through the inductor in clockwise direction and will create a magnetic field. Therefore, the inductor will store some energy and in this moment the diode is not conducting. When the switch opens, the current will flow to the diode and the magnetic field previously created will be eliminated to maintain the current towards the load.

There are two operating modes for boost converters: i) continuous conduction mode (CCM) and ii) discontinuous conduction mode (DCM). The circuit operates in CCM if i_L does not reach zero during all the period and it operates in DCM if i_L is zero during part of the switching period [18].

Some important Equation that describe the boost working principle are the following:

Continuous Conduction Mode

- Output Voltage (V):

$$V_O = \frac{V_I}{1 - D} \quad (1)$$

- Inductor Current (A):

$$\bar{I}_L = \frac{1}{2} \frac{V_I}{L} DDT + \frac{1}{2} \frac{V_I - V_O}{L} (1 - D)DT \quad (2)$$

- Efficiency (%):

$$\eta = 1 - \frac{V_S}{V_I} D - \frac{V_D}{V_O} \quad (3)$$

- Output Voltage Ripple (V):

$$\Delta V_O \approx \frac{1}{C} I_O DT = \frac{1}{C} \frac{V_O}{R_L} DT \quad (4)$$

Continuous Conduction Mode Limit

- Operation Mode Limit Condition:

$$\frac{L}{R_L} > \frac{D(1 - D)^2}{2f_{sw}} \quad (5)$$

- Inductor Current (A):

$$\bar{I}_{LB} = \frac{\Delta i_L}{2} = \frac{1}{2} \frac{V_I}{L} DT \quad (6)$$

Discontinuous Conduction Mode

- Output Voltage (V):

$$V_O = \frac{D + D_0}{D_0} V_I \quad (7)$$

- Inductor Current (A):

$$\bar{I}_L = \frac{\Delta I_L}{2} = \frac{\Delta i_L}{2} = \frac{1}{2} \frac{V_I}{L} DT(D + D_0) = \bar{I}_I \quad (8)$$

- D_0 :

$$D_0 = \frac{L}{DRT} \pm \sqrt{\left(\frac{L}{DRT}\right)^2 + \frac{2L}{RT}} \quad (9)$$

2) *Multiple Converters Working Principle*: The main goal of this project is to guarantee a certain voltage amount in order to power up a implantable medical device. The supply is intended to be through the use of multiple boost DC-DC converters that have sensors in their inputs and which will readjust every time a sensor is disconnected or fails. This way, it is needed to assure that the converter's working principle is verified when multiple parallel converters are displayed and also that the voltage amount is maintained.

Since the system has multiple input power sources, each source has one DC-DC boost converter, as show in Figure 3.

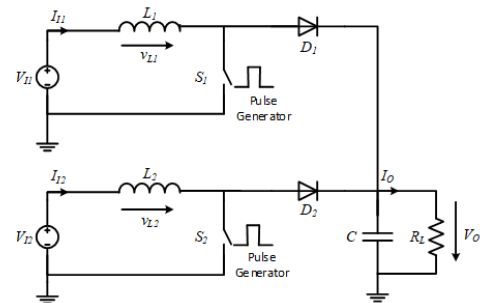


Fig. 3. Multiple parallel DC-DC boost converters sharing a same load.

The general circuit working principle is very similar to the previous described boost DC-DC converter working principle. For this analysis, two input power sources are considered, V_{I_1} and V_{I_2} , also both diodes, D_1 and D_2 , and switches, S_1 and S_2 , which are considered as ideal and the resistance R_L represents the load.

For studying the steady state behavior of the two converters working simultaneously and considering that each one, when working alone, has two operation modes (continuous and discontinuous conduction mode), it is considered the existence of three combinations, based on the converter's individual working principle, which are:

- Both converters in continuous conduction mode, CCM-CCM;
- Both converters in discontinuous conduction mode, DCM-DCM;
- Upper converter in continuous conduction mode and lower converter in discontinuous conduction mode (or vice versa), CCM-DCM;

Considering the converters sizing and considering that both converters are supposed to be dimensioned for generating the same output voltage, for each mentioned combination, there are the following scenarios:

- 1) $V_{I_1} > V_{I_2}$ and $V_{O_1} = V_{O_2}$;
- 2) $V_{I_1} = V_{I_2}$ and $V_{O_1} = V_{O_2}$;
- 3) $V_{I_1} < V_{I_2}$ and $V_{O_1} = V_{O_2}$.

In order to be able to study the behavior of the converters' set, the previous mentioned sizing will be simulated and a steady state analysis of the simulation results will be done. Also, a prevision of the general working principle of the converters' set will be held through the simulation results.

Continuous-Continuous Conduction Mode: For the existence of this operation mode, it is needed to guarantee that continuous conduction mode is verified when individually sizing the converters. This way, considering Equation 5, a set of possible parameters is presented in Table II.

TABLE II
PARAMETERS FOR CONTINUOUS CONDUCTION MODE.

Commuting Frequency, f_{sw}	10 kHz
Capacitance, C	500 μ F
Load, R_L	10 Ω

Taking into account the converters' individual sizing resulting scenarios for this operation mode, some possible parameters are presented in Table III, considering Equations 1 and 5. It was considered that the switches duty cycle were synchronized instead of complementary, since there is no difference once the diodes don't conduct in reverse bias and $V_O > \forall V_I$, so one input's the inductor current will never flow backwards and will never interfere with another input.

The corresponding steady state simulations for Scenario 1, 2 and 3 with both converters in CCM, working simultaneously, are shown in Figure 4.

TABLE III
CONVERTERS SIZING FOR CONTINUOUS CONDUCTION MODE, AT START (WHEN WORKING INDIVIDUALLY).

		Scenario 1 $V_{I_1} > V_{I_2}$	Scenario 2 $V_{I_1} = V_{I_2}$	Scenario 3 $V_{I_1} < V_{I_2}$
Converter 1	Input Voltage, V_{I_1}	0.7 V	0.7 V	0.35 V
	Duty cycle, D_1	50%	50%	75%
	Inductor Average Current, \bar{I}_{L_1}	48.6 mA	48.6 mA	37.5 mA
	Inductor, L_1	0.36 mH	0.36 mH	0.36 mH
Converter 2	Input Voltage, V_{I_2}	0.35 V	0.7 V	0.7 V
	Duty cycle, D_2	75%	50%	50%
	Inductor Average Current, \bar{I}_{L_2}	37.5 mA	48.6 mA	48.6 mA
	Inductor, L_2	0.36 mH	0.36 mH	0.36 mH
Output Voltage, V_O			1.4 V	

From the simulation results, it is possible to verify the steady state behavior of the set, as it is presented in Table IV.

TABLE IV
SIMULATION RESULTS ANALYSIS FOR SCENARIO 1, 2 AND 3 WITH BOTH CONVERTERS ARE SIZED TO GENERATE THE SAME OUTPUT VOLTAGE IN CCM AND WORKING SIMULTANEOUSLY.

		Scenario 1 $V_{I_1} > V_{I_2}$	Scenario 2 $V_{I_1} = V_{I_2}$	Scenario 3 $V_{I_1} < V_{I_2}$
Converter 1	CCM	x ⁽¹⁾	x ⁽²⁾	
	CCM Limit			x ⁽³⁾
Converter 2	CCM		x ⁽²⁾	x ⁽³⁾
	CCM Limit	x ⁽¹⁾		
Inductor Average Current, \bar{I}_L		\bar{I}_{L_1}	$\bar{I}_{L_1} = \bar{I}_{L_2}$	\bar{I}_{L_2}

Analyzing the simulation results and Table IV it is possible to conclude that:

- When $V_{O_1} = V_{O_2}$:
 - The converter corresponding to V_{I_2} operates in the limit of continuous conduction mode, for $V_{I_1} > V_{I_2}$ (situation (1)). Situation (1) is the symmetric of (3).
 - When $V_{I_1} = V_{I_2}$ and $V_{O_1} = V_{O_2}$, both converters contribute with 50% for the output voltage, as presented in situation (2).
- The converter that enforces the output voltage is the master and it's the one that, when working alone, generates the higher output current and has higher inductor average current.
 - The slave converter will contribute with the minimum amount of current.

Considering that both converters are working simultaneously and share the same load, the necessary power to supply the load will be divided through both converters,

$$V_{I_1} \bar{I}_{I_1} + V_{I_2} \bar{I}_{I_2} = V_O I_O. \quad (10)$$

The output voltage, V_O , is supposed to be constant, which implies that I_O has to be constant, and consequently

$$V_{I_1} \left(\bar{I}_{I_1} + \frac{V_{I_2} \bar{I}_{I_2}}{V_{I_1}} \right) = \frac{V_O^2}{R_L} \quad (11)$$

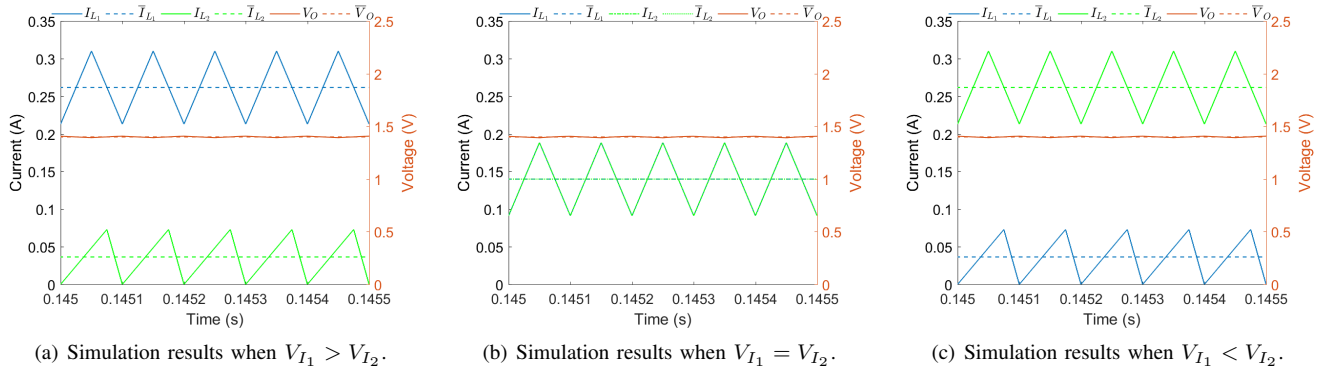


Fig. 4. Simulation results for Scenario 1, 2 and 3 when $V_{O1} = V_{O2}$ and both converters are in CCM.

also has to be constant. This means that in the presence of a current, \bar{I}_{I2} , \bar{I}_{I1} drops apart from $\frac{V_{I2}\bar{I}_{I2}}{V_{I1}}$ and it is possible to conclude that is the total of the average currents that remain constant.

However, if $V_{I1} \gg V_{I2}$, from Equation 10 results that $V_{I1}\bar{I}_{I1}$ must be constant, which means that the current regime in L_1 slightly decreases its average value and in L_2 , as D is the same, result a smaller V_{O2} . This happens due to decreases until discontinuous operating mode, where the value of $(1-D)$ is such that

$$V_{I2} \frac{\Delta i_{L2}}{2} (D + D_0) = \frac{V_{O2}^2}{R_L}, \quad (12)$$

$$\Delta i_{L2} = \frac{V_{I2}}{L_2} DT. \quad (13)$$

If V_{I1} drops its value, V_O decreases, according to $V_O = \frac{V_{I1}}{1-D}$, until reaching the previous V_{O2} value. In this moment, I_{L2} starts commanding and V_O remains in V_{O2} .

Assuming that both converters are sized to generate the same output voltage individually, it is already known that one converter will behavior as master and the other as slave for all the considered scenarios and situations. This way, making use of Equation 10, knowing that $I_O = \frac{V_O}{R_L}$, and Equations 2 for the upper converter and 6 for the lower converter, it is possible to describe the converters simultaneous behavior in steady state,

$$\begin{cases} \frac{V_O^2}{R_L} = V_{I1}\bar{I}_{I1} + V_{I2}\bar{I}_{I2} \\ \bar{I}_{I1} = \frac{1}{2} \frac{V_{I1}}{L_1} D_1 T + \bar{I}_{Off} \\ \bar{I}_{I2} = \frac{1}{2} \frac{\Delta i_{L2}}{2} = \frac{1}{2} \frac{V_{I2}}{L_2} D_2 T \\ V_O = \frac{V_{I1}}{1-D_1} \end{cases} \quad (14)$$

Considering the steady state behavior of the set with both converters working simultaneously, since the upper converter is the one that has the higher \bar{I}_L , it will be the master and will enforce the output voltage of the set, $V_O = V_{O1} = 1.4$ V. The lower converter will behave as a slave and contribute with the minimum output current. The converters are sized to generate the same amount of voltage and with the values of

the scenario 1 and Table II, so the lower converter will be at the limit of continuous conduction mode.

Taking the solutions found in the system of equations 14, for the parameters of this example, the values obtained are

$$\begin{cases} V_O = 1.4 \text{ V} \\ \bar{I}_{I1} = 262 \text{ mA} \\ \bar{I}_{Off} = 213 \text{ mA} \\ \bar{I}_{I2} = 36.4 \text{ mA} \end{cases} \quad (15)$$

These values confirm the conclusions mentioned before and comply with the values obtained in Figure 4(a).

Discontinuous-Discontinuous Conduction Mode: For the steady state analysis of this operation mode, it is needed to guarantee that discontinuous conduction mode is verified when individually sizing the converters. This way, considering Equation 5, the parameters presented in Table V are considered.

TABLE V
PARAMETERS FOR DISCONTINUOUS CONDUCTION MODE.

Commuting Frequency, f_{sw}	10 kHz
Capacitance, C	500 μ F
Load, R_L	100 Ω

Taking into account the converters' individual sizing resulting scenarios for this operation mode, some possible parameters are presented in Table VI, considering Equations 5,7 and 9.

The corresponding steady state simulations for Scenario 1, 2 and 3, when both converters are sized to operate in DCM and working simultaneously, are shown in Figure 5.

From the simulation results, it is possible to verify the steady state behavior of the set, as it is presented in Table VII.

Analyzing the simulation results and Table VII it is possible to conclude that when converters are working simultaneously in steady state:

- The output voltage of the set, V_O depends on both converters contribution, so a typical master-slave topology cannot be applied in this case.

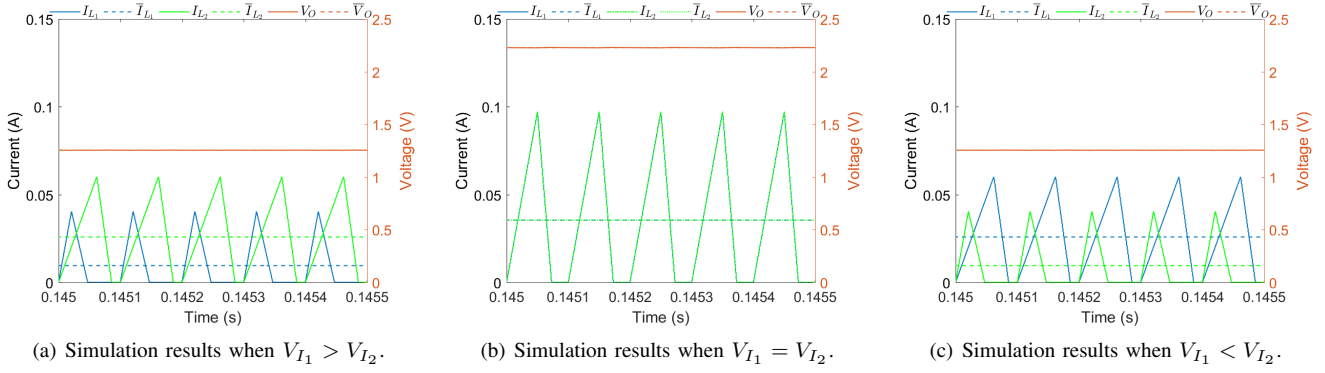


Fig. 5. Simulations results for Scenario 1, when $V_{O1} = V_{O2}$ and both converters are in DCM.

TABLE VI
CONVERTERS SIZING FOR DISCONTINUOUS CONDUCTION MODE, AT
START (WHEN WORKING ALONE).

		Scenario 1 $V_{I1} > V_{I2}$	Scenario 2 $V_{I1} = V_{I2}$	Scenario 3 $V_{I1} < V_{I2}$
Converter 1	Input Voltage, V_{I1}	0.7 V	0.7 V	0.35 V
	Duty cycle, D_1	21%	50%	62%
	D_{O1}	49%	35%	33%
	Inductor Average Current, \bar{I}_{L1}	14.3 mA	20.6 mA	41.3 mA
	Inductor, L_1	0.36 mH	0.36 mH	0.36 mH
Output Voltage, V_{O1}		1 V	1.7 V	1V
Converter 2	Input Voltage, V_{I2}	0.35 V	0.7 V	0.7 V
	Duty cycle, D_2	62%	50%	50%
	D_{O2}	21%	35%	49%
	Inductor Average Current, \bar{I}_{L2}	28.6 mA	41.3 mA	14.3 mA
	Inductor, L_2	0.36 mH	0.36 mH	0.36 mH
Output Voltage, V_{O2}		1 V	1.7 V	1V

TABLE VII
SIMULATION RESULTS ANALYSIS FOR SCENARIO 1, 2 AND 3 WITH BOTH
CONVERTERS IN DISCONTINUOUS CONDUCTION MODE AND WORKING
SIMULTANEOUSLY.

		Scenario 1 $V_{I1} > V_{I2}$	Scenario 2 $V_{I1} = V_{I2}$	Scenario 3 $V_{I1} < V_{I2}$
Converter 1	DCM	x (1)	x (2)	x (3)
Converter 2	DCM	x (1)	x (2)	x (3)
Inductor Average Current, \bar{I}_{L2}		\bar{I}_{L1}	$\bar{I}_{L1} = \bar{I}_{L2}$	\bar{I}_{L2}

- The output voltage of the set, V_O , is higher than any single converter output voltage V_{O1} or V_{O2}
- When any converter is disconnected, the value of the output voltage of the set will go down.
- The converter that has the higher inductor average current contributes with more current, and consecutively, contributes more to the set's output voltage.

- When $V_{O1} = V_{O2}$ and $V_{I1} > V_{I2}$, $\Delta i_{L1} < \Delta i_{L2}$, as shown in situation (1). Symmetrically, when $V_{I1} < V_{I2}$, $\Delta i_{L1} > \Delta i_{L2}$, as presented in situation (3). If $V_{I1} = V_{I2}$, $\Delta i_{L1} = \Delta i_{L2}$, as situation (2) shows.

Considering that both converters are working simultaneously and share the same load, the necessary power to supply the load will be divided through both converters. Assuming that both converters are dimensioned to generate the same

output voltage individually with the values of scenario 1, it is already known that both converters will contribute to the output current. This way, making use of Equation 10, knowing that $I_O = \frac{V_O}{R_L}$ and Equations 8 and 7, applied for each converter, it is possible to describe the converters simultaneous steady state behavior and to predict the set's output voltage,

$$\begin{cases} \frac{V_O^2}{R_L} = V_{I1} \bar{I}_{L1} + V_{I2} \bar{I}_{L2} \\ I_{L1} = \frac{1}{2} \frac{V_{I1}}{L_1} D_1 T (D_1 + D_{O1}) \\ I_{L2} = \frac{1}{2} \frac{V_{I2}}{L_2} D_2 T (D_2 + D_{O2}) \end{cases} \quad (16)$$

Taking the solutions found in the system of equations 16, for the parameters of this example, the values obtained are

$$\begin{cases} V_O = 1.42 \text{ V} \\ \bar{I}_{L1} = 14.29 \text{ mA} \\ \bar{I}_{L2} = 28.63 \text{ mA} \end{cases} \quad (17)$$

As concluded before, both converters contribute to the output voltage of the set which results in a higher value than V_{O1} and V_{O2} . The lower converter will contribute more, since it has a higher \bar{I}_{L2} .

These values confirm the conclusions mentioned before and comply with the values obtained in Figure 5(a).

Continuous-Discontinuous Conduction Mode: For the steady state analysis of this operation mode, it is intended to dimension one converter to operate in continuous conduction mode and the other in discontinuous conduction mode, when individually sizing the converters. It doesn't matter the order of the converter, since their operation is independent of their positioning, so it will be considering that the upper converter (converter 1) will be operating in CCM and the lower one (converter 2) in DCM. This way, considering Equation 5, the parameters presented in Table VIII are considered.

TABLE VIII
PARAMETERS FOR CONTINUOUS-DISCONTINUOUS CONDUCTION MODE.

Commuting Frequency, f_{sw}	10 kHz
Capacitance, C	500 μ F
Load, R_L	10 Ω

Taking into account the converters' individual sizing resulting scenarios for this operation mode, some possible parameters are presented in Table IX, considering Equations 1, 5, 7 and 9.

TABLE IX
CONVERTERS SIZING FOR CONTINUOUS-DISCONTINUOUS CONDUCTION MODE, AT START (WHEN WORKING INDIVIDUALLY).

		Scenario 1 $V_{I1} > V_{I2}$	Scenario 2 $V_{I1} = V_{I2}$	Scenario 3 $V_{I1} < V_{I2}$
Converter 1	Input Voltage, V_{I1}	0.7 V	0.5 V	0.35 V
	Duty cycle, D_1	50%	64%	75%
	Inductor Average Current \bar{I}_{L1}	37.5 mA	48.6 mA	48.6 mA
	Inductor, L_1	0.36 mH	0.36 mH	0.36 mH
Converter 2	Input Voltage, V_{I2}	0.5 V	0.5 V	0.5 V
	Duty cycle, D_2	60%	60%	60%
	D_{02}	33%	33%	33%
	Inductor Average Current \bar{I}_{L2}	387.5 mA	387.5 mA	387.5 mA
	Inductor, L_2	0.036 mH	0.036 mH	0.036 mH
Output Voltage, V_O		1.4 V		

The corresponding steady state simulations for Scenario 1, 2 and 3, when converters are operating in CCM and DCM and working simultaneously, are shown in Figure 6.

From the steady state simulation results, it is possible to verify the behavior of the set, as it is presented in Table X.

TABLE X
SIMULATION RESULTS ANALYSIS FOR SCENARIO 1, 2 AND 3 WITH CONVERTERS IN CONTINUOUS-DISCONTINUOUS CONDUCTION MODE, WITH CONVERTERS WORKING SIMULTANEOUSLY.

		Scenario 1 $V_{I1} > V_{I2}$	Scenario 2 $V_{I1} = V_{I2}$	Scenario 3 $V_{I1} < V_{I2}$
Converter 1	DCM	x (1)	x (2)	x (3)
	Higher Inductor			
Converter 2	DCM	x (1)	x (2)	x (3)
	Average Current \bar{I}_L	\bar{I}_{L2}	\bar{I}_{L2}	\bar{I}_{L2}

Analyzing the steady state simulation results and Table X it is possible to conclude that:

- When $V_{O1} = V_{O2}$ the converter 1 starts to behave like it is operating in discontinuous conduction mode and the behavior of the converter's set is the same as presented in subsection III-A2, as illustrated in situations (1), (2), (3).

From the analysis of Table X, considering the steady state behavior of the set with both converters working simultaneously and with the values of the scenario 1 and Table VIII, it is possible to conclude that both converters will work in DCM.

Taking the solutions Systems of Equations 16, for the parameters of this example, the values obtained are

$$\begin{cases} V_O = 1.509 \text{ V} \\ \bar{I}_{I1} = 48.6 \text{ mA} \\ \bar{I}_{I2} = 387.5 \text{ mA} \end{cases} \quad (18)$$

These values confirm the conclusions mentioned before and comply with the values obtained in Figure 6(a).

As concluded before, this behavior is very similar to the discontinuous-discontinuous conduction mode, so both converters contribute to the output voltage of the set which results in a higher value than V_{O1} and V_{O2} , but the lower converter will contribute more, since it has a higher \bar{I}_{I2} .

Conclusions: From the previous converter behavior steady state analysis, it is possible to conclude that, as the main goal of this work is to generate a certain amount of voltage to power up an IMD, the set of converters sizing has to guarantee the required amount specially when the system has to readjust to solve any input source failure.

Within the three analyzed topologies, only the CCM-CCM topology maintains the output voltage when there are several input sources contributing, contrarily to either DCM-DCM or CCM-DCM, which output voltage depends on the converters and its operation mode. This means that if one source fails the output voltage may either increase or decrease its value, which is not the desired result. So, it is needed to guarantee that the converters are always operating in CCM and considering Equation 5, it is necessary to set an inductor value that ensures the desired behavior for the employed duty cycle values, once that the operating frequency and the load value are fixed.

B. System Architecture

Until now, the set of converters has been dimensioned for standard parameters in order to understand its general steady state behaviour, As previously mentioned, this project intends to be a redundant system for the human body's energy harvesting technique to power an IMD, namely a pacemaker. This means that, in order to study the behaviour as realistically as possible, the system has to be correctly sized in terms of internal components, external load and output power.

Load Impedance: Taking as example the Vitatron E10 S Single Chamber Pacemaker System and its specification [19], it is possible to gather some relevant information about its battery for circuit sizing, as presented in Table XI.

TABLE XI
VITATRON PACEMAKER BATTERY RELEVANT PARAMETERS.

Battery Voltage	Impedance Reference	Average Projected Capacity	Longevity
2.8 V	500 Ω	0.92 Ah	10.4 years

From literature, the impedance of a pacemaker varies from, at least, 200 to 4000 Ω and pacemaker batteries must be designed to cover this value. In the beginning of life, batteries are projected to less than 1 k Ω impedance and over the years the impedance tends to get higher and the current drain lower until it is time to renew it. The capacity of the battery is the estimated amount of current that can be delivered to the load over time. For this example, a 0.92 Ah capacity means that with a load of 500 Ω , the battery is capable of deliver 0.92 A per hour. As the longevity is presented as being 10.4 years, from

$$Time = \frac{Q}{I}, \quad (19)$$

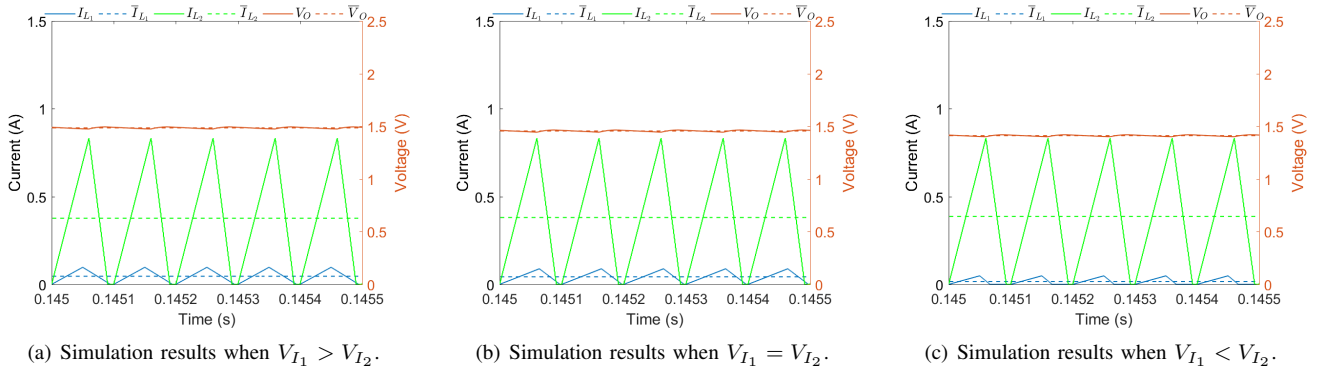


Fig. 6. Simulations results for Scenario 1, when $V_{O_1} = V_{O_2}$ and one converter is in CCM and the other in DCM.

where Q represents the battery capacity, in Ah, and I represents the current drain, in A, by replacing values it is possible to determine that it is delivered to the pacemaker a current drain of about $10 \mu\text{A}$. Also, from [20] the power consumption value of a pacemaker is between $10\text{-}40 \mu\text{W}$.

Inductor Value: Regarding the converters' set behaviour, it is already known from the conclusions of Section III-A2 that to guarantee the necessary voltage amount (in this case, at least, 2.8 V) when readjusting the input sources, the system has to be dimensioned to operate in CCM for all the converters' duty cycle. This way, for a two converters' example, taking Equation 5 and considering a duty cycle of 25% and 50%, it is possible to determine the minimum value inductance for which the system behaves in CCM,

$$L_{min} > \frac{D_{min}(1 - D_{min})^2}{2f_{sw}} R = 0.18 \text{ mH}. \quad (20)$$

However, as concluded on Section III-A2, in order to guarantee the converters behaviour when multiple converters are operating, the value of the inductance has to be higher than the CCM limit. This way, it was considered a value of 0.68 mH .

Output Capacitor: Concerning the output capacitor, from Equation 4 it is possible to determine the minimum value of its capacitance and considering 50 mV as ΔV_O ,

$$C_{min} = \frac{I_{O_{MAX}} D_{MAX}}{f_{sw} \Delta V_O} = 0.36 \mu\text{F}. \quad (21)$$

Input Voltage Sources: Regarding the input voltage, taking Equation 1, to achieve this value, knowing that the converters have to be operating at CCM and with a considered 3 V output voltage goal, the input voltages for converters 1 and 2, if they were working alone, have to be 2.25 V and 1.5 V , respectively.

For the simultaneous operation, System of Equations 14 and its solution, have to be considered. Replacing the correspondent values, the obtained solution is

$$\begin{cases} V_O = 3 \text{ V} \\ \bar{I}_{I_1} = 5.21 \text{ mA} \\ \bar{I}_{O_{ff}} = 0.621 \text{ mA} \\ \bar{I}_{I_2} = 2.76 \text{ mA} \end{cases} \quad (22)$$

The previous results conclude that the input voltage values considered are valid to use for obtaining an output voltage of 3 V .

The input voltage is intended to be collected from two different energy harvesting methods with eventually their corresponding voltage elevator circuit. The chosen methods were the piezoelectric and electrostatic energy harvesters which are able to generate a output voltage of 1.58 V and 2.28 V , respectively.

Schottky Diodes and MOSFET: Since it is intended to simulate the system as realistic as possible, the components that have been considered as ideals until now, namely switches and diodes, have to be substituted for real components. This way, concerning the diode selection, in order to get a voltage drop as low as possible, a Schottky diode has been chosen, namely the 1n5817 one. Regarding the switches, they can be substituted by MOSFETs, namely the Si8424DB one.

Duty Cycle Generator: In order to generate the different duty cycles, it is intended to implement a LMC555 CMOS Timer in each converter in order to generate the supposed duty cycle values.

Zener Diode: As the principle of this project is to set a fixed CD output voltage with value of 3 V , it is needed to force down any higher peak voltage to maintain this value. To do that, a zener diode with a 4 V zener voltage is introduced and placed in anti-parallel with the load.

Due to the increase of current that flows through the zener diode in inverse conduction mode, a 0.3Ω resistor has been placed in series with the capacitor to decrease the amount of current.

C. Dimensioned Circuit

The dimensioned circuit is presented in Figure 7 and the correspondent components values are presented in Table XII.

The correspondent converters set behaviour has been simulated and the results are shown in Figure 8.

As expected, the behaviour corresponds to one reported in conclusions of Section III-A2: the higher average inductor current source takes the command of the output voltage, behaving as the master and the slave is at the limit of his CCM operation. Another conclusion that must be taken into

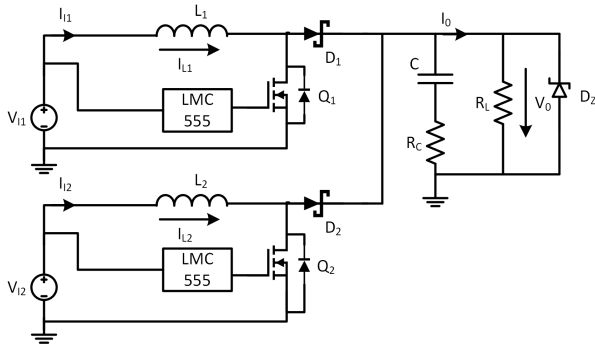


Fig. 7. Multiple converters topology sized circuit.

TABLE XII
PARAMETERS FOR CCM-CCM CONVERTERS SIZING EXAMPLE.

	Upper Converter	Lower Converter
Input Voltage, V_I	$V_{I1}=2.25$ V	$V_{I2}=1.5$ V
Duty Cycle, D	$D_1=25\%$	$D_2=50\%$
Inductance, L	$L_1=0.68$ mH	$L_2=0.68$ mH
Schottky Diode Threshold Voltage, $V_{D_{th}}$	$V_{D1Th}=0.144$ V	$V_{D2Th}=0.144$ V
Commuting Frequency, f_{sw}	200 kHz	
Capacitance, C	0.36 F	
Capacitor Resistor, R_C	0.3 Ω	
Load, R_L	500 Ω	
Zener Diode Voltage, V_{DZ}	4 V	

account is that the previously presented circuit sizing has been succeeded, at least, in respect to the output voltage, which is less than the projected value (3 V), due to the 0.144 V voltage drop at the diode.

IV. CIRCUIT PERFORMANCE IN CASE OF FAILURE

So far, the proposed circuit has been dimensioned in order to obtain a certain amount of voltage when the input sources are working. As the main goal of this work is to design a redundant circuit, capable of readjusting its input sources in case of a failure, it is needed to simulate their failures in order to confirm the desired behaviour.

Concerning the proposed system, when all human body motion harvesters are working and supplying the chosen implantable medical device for this analysis, a pacemaker, it has already been seen that the behaviour of the system can be easily described making use of System of Equations 14. The worrying situation is the system's response in case of any input source failure. Ideally, the system should be capable to readjust its input in such a way that a working input source ensures the desired behaviour and the required output voltage.

If an input voltage source fails, none current will flow through its correspondent inductor and therefore converter, so the output voltage of that converter will be 0 V. Considering System of Equations 14, if a failure is simulated it is possible to induce that the output voltage will be assured only by

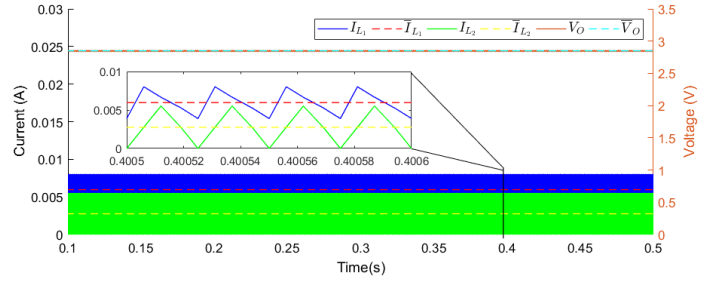


Fig. 8. Time diagram of output voltage, V_O , and inductors current in a two converters' system.

converter 2, resulting in a System of Equations as

$$\begin{cases} \frac{V_O^2}{R_L} = V_{I2} \bar{I}_{I2} \\ \bar{I}_{I2} = \frac{1}{2} \frac{V_{I2}}{L_2} D_2 T \\ V_O = \frac{V_{I2}^2}{1-D} \end{cases} \quad (23)$$

As the output voltage and load is supposed to remain the same, it will be the average inductor current of L_2 that increases.

In order to test if the system corresponds to the previous described expected behavior, a piecewise linear voltage source is introduced and placed as V_{I1} and V_{I2} , respectively.

This way, using the circuit sizing parameters presented in Table XII and implementing the piecewise linear voltage generator in each input, with $V_{I1} = 2.25$ V and $V_{I2} = 1.5$ V amplitudes and an operating frequency of 5 Hz, it is possible to analyze the system's behaviour and test the viability of this solution.

Regarding to the expected behaviour, concerning the output voltage, it is expected to see a DC value of 3 V with possible voltage breaks at the moment of input sources' readjustment. This means that, when both sources are working, the behaviour has to correspond to the one analyzed in Section III-A2, since both converters are operating in CCM. It is also expected that the upper converter (converter 1) begins to behave as the master, once it has a higher average inductor current value, and the lower converter to behave as slave. When the master fails, its inductor current reaches 0 A after 10 ms, the converter 2 is expected to start behaving as master (since it is the only working converter) and to increase its average inductor current, in order to maintain the output voltage value. It is in this transition that may occur momentary voltage breakdowns, which are expected to return to the supposed value passed a few ms. The simulation results are presented in Figure 9.

Analyzing these results, it is possible to conclude that the previously described behaviour is assured and the stability of nearly 3 V output voltage is guaranteed.

This failure study was also done for a three converters system and the results were consistent with the ones obtained for the two converters example.

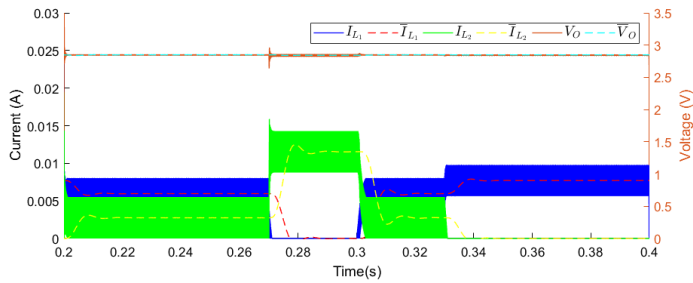


Fig. 9. Time diagram of output voltage, V_O , and inductors current when a failure occurs in a two converters' system.

V. CONCLUSION

Taking advantage of the energy harvesting devices, such as piezoelectric or electrostatic generators, which gather the best characteristics among other ones, and combining them as multiple input sources may be a reliable solution of powering IMDs. Although most of these devices are usually low powered, it is needed to boost the generated voltage, using voltage elevation circuits for this purpose. However, when using these generators, their continuous working status cannot always be assured.

In this work, a system capable of conditioning the collected voltage from energy harvesters to power up an IMD is proposed. This system that, being very simple, besides elevating the several sources voltages, automatically guarantees the existence of a working input power source has been developed and optimized for a real pacemaker's example. To achieve that, a detailed study about simultaneous behaviour of multiple DC-DC converters has been done in order to achieve the best sizing for this project goal. Ultimately, it has been proved that this system is capable of self-readjusting the input voltage source into a permanent working one without compromising the circuit performance and fulfilling the energy requirements of the considered pacemaker.

Future work can be directed to a better simulation of the scavenging sensors or devices, in order to accomplish a more global and realistic simulation for the prototype. Also, an integrated prototype should be considered because it is the usual technology used in implants and so a more accurate behaviour could be checked out.

REFERENCES

- [1] N. Mano, F. Mao, and A. Heller, "Characteristics of a miniature compartment-less glucose-O₂ biofuel cell and its operation in a living plant," *Journal of the American Chemical Society*, vol. 125, no. 21, pp. 6588–6594, 2003.
- [2] Y. Yang, X.-J. Wei, and J. Liu, "Suitability of a thermoelectric power generator for implantable medical electronic devices," *Journal of Physics D: Applied Physics*, vol. 40, no. 18, pp. 5790–5800, 2007. [Online]. Available: <http://stacks.iop.org/0022-3727/40/i=18/a=042?key=crossref.3be06556157bb503f0c2fdf1c77a3403>
- [3] J. A. Nagel, I. Sieber, U. Gengenbach, H. Guth, G. Bretthauer, and R. F. Guthoff, "Investigation of a thermoelectric power supply for the artificial accommodation system," *2010 3rd International Symposium on Applied Sciences in Biomedical and Communication Technologies, ISABEL 2010*, pp. 0–4, 2010.
- [4] V. Luciano, E. Sardini, and M. Serpelloni, "An electromechanical generator implanted in human total knee prosthesis," *Lecture Notes in Electrical Engineering*, vol. 162 LNEE, pp. 25–30, 2014.
- [5] A. Nasiri, S. A. Zabalawi, and D. C. Jeutter, "A linear permanent magnet generator for powering implanted electronic devices," *IEEE Transactions on Power Electronics*, vol. 26, no. 1, pp. 192–199, 2011.
- [6] R. Morais, N. M. Silva, P. M. Santos, C. M. Frias, J. A. Ferreira, A. M. Ramos, J. A. Simes, J. M. Baptista, and M. C. Reis, "Double permanent magnet vibration power generator for smart hip prosthesis," *Sensors and Actuators, A: Physical*, vol. 172, no. 1, pp. 259–268, 2011. [Online]. Available: <http://dx.doi.org/10.1016/j.sna.2011.04.001>
- [7] R. Tashiro, N. Kabei, H. Kotera, K. Katayama, Y. Ishizuka, F. Tsuboi, and K. Tsuchiya, "Development of an Electrostatic Generator that Harnesses the Motion of a Living Body. Generation Using Heartbeat," *Transactions of the Japan Society of Mechanical Engineers Series C*, vol. 67, no. 659, pp. 2307–2313, 2001.
- [8] R. Tashiro, N. Kabei, K. Katayama, F. Tsuboi, and K. Tsuchiya, "Development of an electrostatic generator for a cardiac pacemaker that harnesses the ventricular wall motion," *Journal of Artificial Organs*, vol. 5, no. 4, pp. 239–245, 2002.
- [9] P. Miao, P. D. Mitcheson, A. S. Holmes, E. M. Yeatman, T. C. Green, and B. H. Stark, "Mems inertial power generators for biomedical applications," *Microsystem Technologies*, vol. 12, no. 10-11, pp. 1079–1083, 2006.
- [10] S. Almouahed, M. Gouriou, C. Hamitouche, E. Stindel, and C. Roux, "The use of piezoceramics as electrical energy harvesters within instrumented knee implant during walking," *IEEE/ASME Transactions on Mechatronics*, vol. 16, no. 5, pp. 799–807, 2011.
- [11] B. E. Lewandowski, K. L. Kilgore, and K. J. Gustafson, "Design considerations for an implantable, muscle powered piezoelectric system for generating electrical power," *Annals of Biomedical Engineering*, vol. 35, no. 4, pp. 631–641, 2007.
- [12] M. Deterre, E. Lefeuvre, Y. Zhu, M. Woytasik, B. Boudaud, and R. D. Molin, "Micro blood pressure energy harvester for intracardiac pacemaker," *Journal of Microelectromechanical Systems*, vol. 23, no. 3, pp. 651–660, 2014.
- [13] Z. Chen, M. K. Law, P. I. Mak, and R. P. Martins, "A Single-Chip Solar Energy Harvesting IC Using Integrated Photodiodes for Biomedical Implant Applications," *IEEE Transactions on Biomedical Circuits and Systems*, vol. 11, no. 1, pp. 44–53, 2017.
- [14] A. Khaligh, J. Cao, and Y. Lee, "A Multiple-Input DCDC Converter Topology," *IEEE Transactions on Power Electronics*, vol. 24, no. 3, pp. 862–868, 2009. [Online]. Available: <http://ieeexplore.ieee.org/lpdocs/epic03/wrapper.htm?arnumber=4760221>
- [15] Y. M. Chen, Y. C. Liu, and S. H. Lin, "Double-input PWM DC/DC converter for high-/low-voltage sources," *IEEE Transactions on Industrial Electronics*, vol. 53, no. 5, pp. 1538–1545, 2006.
- [16] L. Kumar and S. Jain, "A multiple source DC/DC converter topology," *International Journal of Electrical Power & Energy Systems*, vol. 51, pp. 278–291, 2013. [Online]. Available: <http://linkinghub.elsevier.com/retrieve/pii/S014206151300080X>
- [17] A. Deihimi, M. E. Seyed Mahmoodieh, and R. Iravani, "A new multi-input step-up DCDC converter for hybrid energy systems," *Electric Power Systems Research*, vol. 149, pp. 111–124, 2017. [Online]. Available: <http://dx.doi.org/10.1016/j.epsr.2017.04.017>
- [18] M. de Medeiros Silva, *Circuitos com transistores bipolares e MOS*, ser. Manuais universitários. Fundação Calouste Gulbenkian. Serviço de Educação e Bolsas, 1999. [Online]. Available: <https://books.google.pt/books?id=3jeZAAAACAAJ>
- [19] Vitatron, "E10S pacemaker specifications," p. 4, 2010. [Online]. Available: <http://www.vitatron.com/downloads/e10-spec.pdf>
- [20] A. Haerberlin, A. Zurbuchen, S. Walpen, J. Schaefer, T. Niederhauser, C. Huber, H. Tanner, H. Servatius, J. Seiler, H. Haerberlin, J. Fuhrer, and R. Vogel, "The first batteryless, solar-powered cardiac pacemaker," *Heart Rhythm*, vol. 12, no. 6, pp. 1317–1323, 6 2015. [Online]. Available: <https://www.sciencedirect.com/science/article/pii/S1547527115002520>